

Oncolytic Vaccinia Virus Expressing the Human Somatostatin Receptor SSTR2: Molecular Imaging after Systemic Delivery Using ^{111}In -Pentetreotide

J. Andrea McCart,^{1,2,*} Navneet Mehta,^{1,3} Deborah Scollard,⁴ Raymond M. Reilly,^{3,4,5} Jorge A. Carrasquillo,⁶ Nan Tang,¹ Hui Deng,¹ Marshall Miller,⁷ Hui Xu,⁷ Steven K. Libutti,⁷ H. Richard Alexander,⁷ and David L. Bartlett^{7,†}

¹Division of Experimental Therapeutics, Toronto General Research Institute, Toronto, ON, Canada M5G 2M1

²Department of Surgery, ³Department of Pharmaceutical Sciences, and ⁵Department of Medical Imaging, University of Toronto, Toronto, ON M5G 1V7, Canada

⁴Division of Nuclear Medicine, Toronto General Hospital, Toronto, ON M5G 2C4, Canada

⁶Department of Nuclear Medicine, Warren G. Magnuson Clinical Center and ⁷Surgery Branch, National Cancer Institute, National Institutes of Health, Bethesda, MD 20892, USA

*To whom correspondence and reprint requests should be addressed at Toronto General Research Institute, 67 College Street, Room 4-408, Toronto, ON, Canada M5G 2M1. E-mail: amccart@uhnres.utoronto.ca.

Available online 24 July 2004

Oncolytic vaccinia viruses (VV) have demonstrated tumor specificity, high levels of transgene expression, and anti-tumor effects. The ability to visualize vector biodistribution noninvasively will be necessary as gene therapy vectors come to clinical trials, and the creation of a VV that can both treat tumors and permit noninvasive imaging after systemic delivery is therefore an exciting concept. To facilitate imaging, a VV expressing the human somatostatin receptor type 2 (SSTR2) was created. Cells infected with the SSTR2-expressing VV or controls were incubated with the somatostatin analog ^{111}In -pentetreotide with or without an excess of nonradiolabeled pentetreotide. The SSTR2-infected cells bound ^{111}In -pentetreotide sixfold more efficiently than control virus-infected cells and this binding was specifically blocked by nonradiolabeled pentetreotide. Nude mice bearing subcutaneous murine colon CA xenografts were injected intraperitoneally with the SSTR2-expressing VV or control VV. After 6 days, mice were injected with ^{111}In -pentetreotide and imaged. Mice were sacrificed and organs collected and counted in a gamma counter. The uptake of radioactivity in tumors and normal tissues (percentage injected dose per gram) and tumor-to-normal tissue ratios were determined. Tumors infected with the SSTR2-expressing VV accumulated significantly higher concentrations of radioactivity compared to tumors in animals receiving the control virus. SSTR2-infected tumors were visible on imaging 6 days after VV injection and could be visualized for up to 3 weeks post-viral injection using repeat injections of ^{111}In -pentetreotide. This reporter gene imaging strategy could be a very effective method to visualize vector distribution, expression, and persistence over time and enhances the potential of VV as a novel anti-cancer therapeutic.

Key Words: gene therapy, molecular imaging, reporter genes, vaccinia virus, somatostatin receptor

INTRODUCTION

Vaccinia virus (VV) is a cytolitic viral vector that infects and preferentially replicates in rapidly dividing cells and can be readily engineered to express genes in cancer cells [1,2]. This tumor selectivity is thought to be due to two factors: (1) VV requires the substrates present

in dividing cells since it has been engineered without its thymidine kinase gene or vaccinia growth factor genes [3] and (2) VV is a large (>200 nm) molecule. It is difficult for it to extravasate from blood vessels in the absence of "leaky" vasculature such as that present in tumors and ovaries [4,5]. VV's ability to extravasate into tumors *in vivo* has been potentiated by factors such as hyperthermia that

increase vascular leakiness (D. L. Bartlett, unpublished results). We have previously demonstrated a dramatic anti-tumor effect with systemic delivery of this vector in the absence of any therapeutic genes [3].

The characteristics that give vaccinia its remarkable potential as an anti-cancer therapeutic may also make it valuable as an imaging tool. Because the virus preferentially infects and replicates in tumor cells, it leads to a localized amplification of any genes expressed. The protein products of the expressed genes represent targets for functional imaging that when amplified selectively in tumor cells can yield a high tumor-to-background ratio. Noninvasive imaging of VV *in vivo* would have several important applications: (1) biodistribution and persistence studies of the vector as part of a gene therapy follow-up program, (2) detection and monitoring of small-volume disease through introduction of a functional imaging target into cancer cells, and (3) visualization of disease burden in humans to monitor the course and evaluate the efficacy of anti-cancer therapeutics, particularly gene therapy.

As novel gene therapy vectors for cancer progress to clinical trials it will be necessary to track these vectors noninvasively to determine biodistribution and persistence. Two approaches to vector imaging have been employed. Light, either bioluminescent (luciferase) [6–9] or fluorescent (green fluorescent protein) [10,11], can be detected by optical imaging with cooled charge-coupled device cameras. Although this method is very sensitive, limitations exist. Currently it is not available for large animals or humans, is difficult to quantitate, and is limited by the penetration of light, which is restricted to only a few millimeters depth beyond the skin surface. To overcome some of these difficulties, one group is using a combined approach with a fusion protein that can be detected both optically and by nuclear medicine scans [12].

As a second strategy, radiotracers can accumulate in the target tumor or tissue due to the presence of a novel enzyme (e.g., herpes simplex virus thymidine kinase [13–16]), human somatostatin receptor type 2 (SSTR2) [17–19], dopamine D2 receptor [20–22] or transporter such as the sodium iodide symporter [23–25] or dopamine transporter [26]. Several laboratories have utilized these genes delivered in retroviral vectors [13,23,27,28], adenoviral vectors [14,15,20,24,25,29,30], or herpesvirus vectors [16]. While the accumulation of the radiotracers was relatively good in each of these studies, the biggest limitation has been the method of vector delivery. Tumors/target organs were either transduced *ex vivo* [13,28] or injected directly [15,16,25], which may be clinically relevant only in certain scenarios such as prostate cancer.

The SSTR2 is targeted by the high-affinity synthetic peptide pentetreotide, which is commonly used for receptor imaging after being radiolabeled with indium-111 [17]. This receptor is normally expressed in human

kidney cells and neuroendocrine tumors. Gene therapy approaches to deliver the SSTR2 to tumors have been used [19,30–34]. A relatively high level of receptor expression was achieved in the tumor. These studies also used intratumoral viral delivery, rather than systemic, which could be a limitation of gene therapy for a wide variety of human cancers. By using VV to deliver the genes encoding radiopharmaceutical receptors, we avoid these problems because VV will be administered systemically and will track to the tumor(s) of interest.

Here we describe the construction, biodistribution, and imaging potential after systemic delivery of a VV expressing the gene for the SSTR2.

RESULTS

Creation of a Vaccinia Virus Expressing the SSTR2

We recombined the human SSTR2 into our vaccinia shuttle under the control of the VV synthetic late promoter (Fig. 1A) and expanded and purified it as described below. We verified expression of the SSTR2 in cells after infection with the SSTR2-expressing VV using RT-PCR (Fig. 1B) and immunostaining (data not shown). RT-PCR demonstrated the appropriate size band at 1100 bp in the SSTR2-infected cells but not in control-infected cells. No contaminating DNA was seen in the absence of the reverse transcriptase (data not shown).

In Vitro Binding of ¹¹¹In-Pentetreotide to SSTR2-Expressing Cells

To determine if the somatostatin receptor was being specifically produced and appropriately processed we tested the system *in vitro*. After infection of CV1 cells with either the SSTR2-expressing VV or controls at a multiplicity of infection (m.o.i.) of 1, we saw approximately 6-fold higher binding of ¹¹¹In-pentetreotide (Fig. 1C) in cells infected with the SSTR2-expressing virus. Next, we performed a competitive receptor binding assay using increasing concentrations of nonradiolabeled pentetreotide relative to ¹¹¹In-pentetreotide to demonstrate further expression of SSTR2 and to estimate the dissociation constant for binding of the radiopharmaceutical to the receptor. We saw complete inhibition of ¹¹¹In-pentetreotide binding when we added a 25- to 50-fold excess of nonradiolabeled pentetreotide (Fig. 1D). This indicates that (a) the receptor is appropriately processed and expressed on the cell surface, (b) this is specific and not a global “vaccinia” effect, and (c) the receptor can be specifically inhibited by nonradiolabeled pentetreotide.

Imaging of SSTR2-Infected MC38 Tumors

In a more clinically relevant model we imaged tumor-bearing mice after systemic injection of our SSTR2-expressing VV. When subcutaneous MC38 murine colon cancer xenografts were 5 to 7 mm in size, we injected

10^9 plaque-forming units (pfu) of the SSTR2 or control virus intraperitoneally (ip). Six days later we injected 150 μ Ci (0.5–0.7 ng) of 111 In-pentetreotide via the tail vein. We imaged the mice 4 (not shown) and 24 h (Fig. 2) after radiopharmaceutical injection. As expected the tumor-to-background ratio was lower at 4 h and improved at 24 h as the non-receptor-bound radiopharmaceutical was eliminated from the animal. 111 In-pentetreotide accumulated in the kidneys due to uptake of the peptide by proximal renal tubular cells [35]. In the tumors, uptake was seen only in mice injected with the SSTR2-expressing virus. The radioactivity in the tumors persisted for up to 24 h after injection of 111 In-pentetreotide (Fig. 2). No evidence of 111 In-pentetreotide accumulation (as a surrogate of viral infection) was

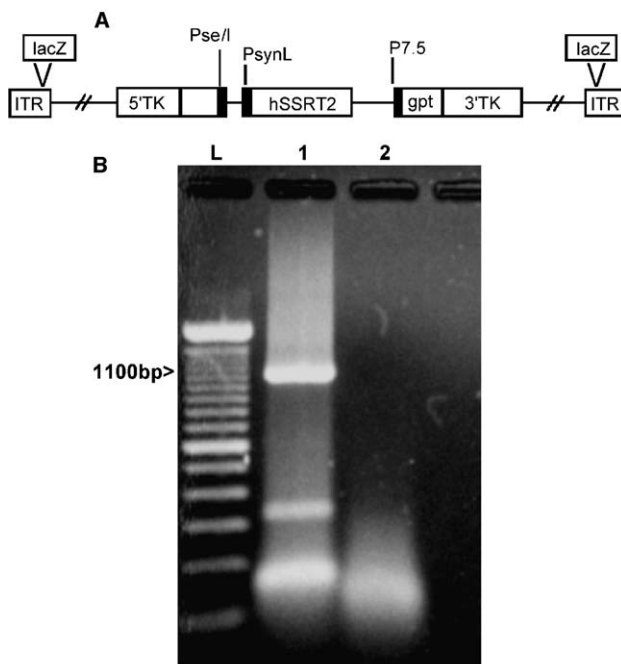


FIG. 1. (A) Linear diagram of vvDD-SSTR2. Sites of left (5TK) and right (3TK) segments of vaccinia thymidine kinase gene, synthetic late promoter (PsynL), synthetic early/late promoter (Pse/I), 7.5 promoter (P7.5), and xanthine-guanine phosphoribosyl transferase (gpt) gene are indicated. The VGF sites within the inverted terminal repeats (ITR) are interrupted by the insertion of the lacZ gene. (B) RT-PCR analysis of CV1 cells infected with the SSTR2-expressing virus (vvDD-SSTR2, lane 1) or control virus (vvDD-GFP, lane 2). Primers for the SSTR2 gene amplify an 1100-bp segment in vvDD-SSTR2 but no band is amplified from the control virus. β -Actin control and no-RT control (for DNA contamination) are not shown. L, 100 bp ladder. (C) Counts per minute 18 h after *in vitro* infection of CV1 cells with no virus, vvDD-SSTR2, or vvDD-GFP and incubation with 111 In-pentetreotide. Only the cells infected with vvDD-SSTR2 specifically bind the 111 In-pentetreotide. (D) Counts per minute 18 h after *in vitro* infection of MC38 cells with vvDD-SSTR2 or vvDD-GFP and incubation with 111 In-pentetreotide and increasing amounts of excess cold pentetreotide. Complete inhibition of binding of 111 In-pentetreotide to the vvDD-SSTR2-infected cells was seen when 25- to 50-fold excess nonradioactive pentetreotide was added.

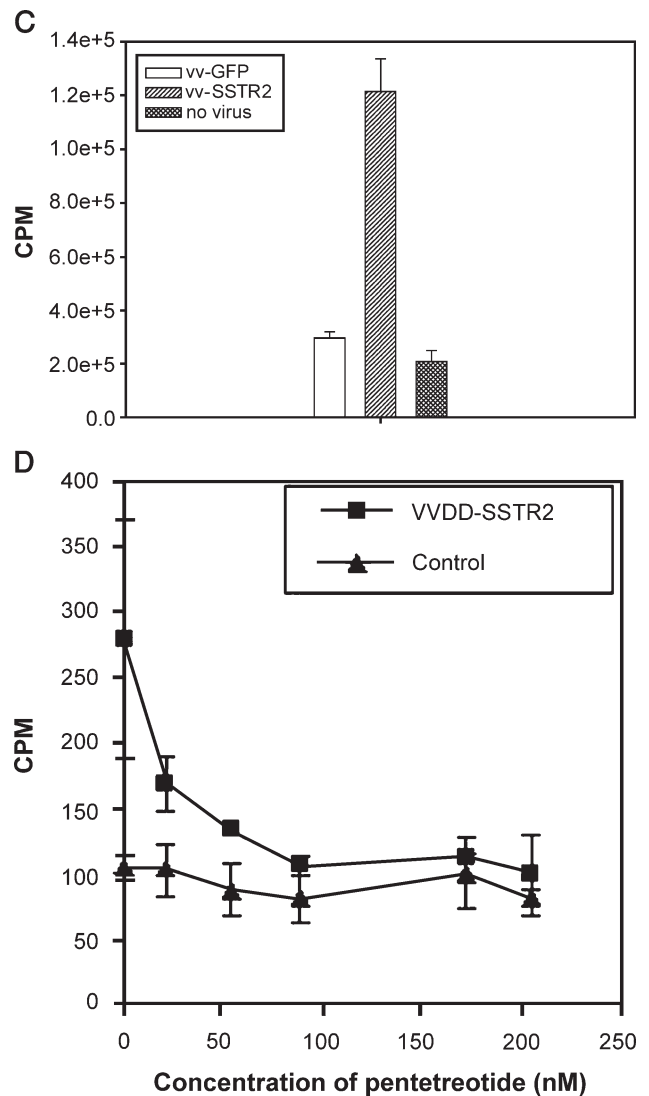


FIG. 1 (continued).

seen in other organs except kidneys as was expected from previous biodistribution studies [2]. We imaged the mice weekly, in each case 24 h after 111 In-pentetreotide injection. Tumors were visualized at 1 (Fig. 2) and 3 (Fig. 3) weeks post-viral infection although, as anticipated due to viral clearance, the intensity of the tumor images at 3 weeks was lower.

Using these images, we manually drew regions of interest (ROIs) around major organs and quantitate the amount of 111 In-pentetreotide uptake noninvasively using counts per pixel as the readout. At 24 h, mice receiving the SSTR2-expressing virus had significantly ($P = 0.04$) higher tumor counts (Table 1) compared to mice receiving the control virus and no significant differences were noted between the other organs.

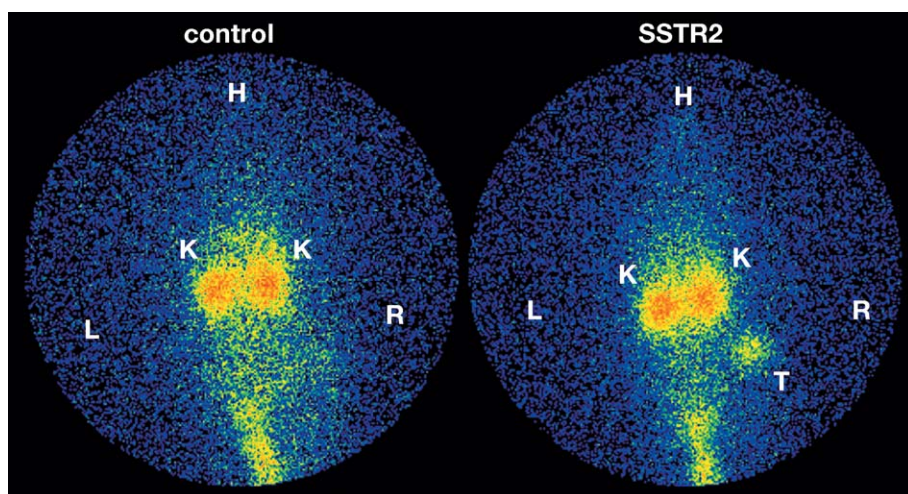


FIG. 2. Posterior whole-body images of tumor-bearing athymic mice 1 week after ip injection with vaccinia virus and 24 h after iv (tail vein) injection with ^{111}In -pentetreotide. Tumor (T) is visible on the right flank of vvDD-SSTR2-injected mouse (right) but not in the control vvDD-GFP-injected mouse (left). Prominent visualization of both kidneys (K) is noted in all animals, as well as the tail (site of injection). The right (R) and left (L) sides of the mouse as well as the head (H) are indicated.

^{111}In -Pentetreotide Biodistribution

To confirm the imaging results we measured the uptake of ^{111}In -pentetreotide in the MC38 xenografts and other tissues after delivery of the SSTR2-expressing VV. We collected and weighed tissues and counted them in a gamma counter at 4 and 24 h after injection with ^{111}In -pentetreotide. We found a significantly greater uptake of radioactivity in the SSTR2-infected tumors compared to that in both control groups (Figs. 4A and 4B). This is consistent with our previous studies in which higher expression of luciferase was seen in MC38 tumor xenografts after systemic delivery of a luciferase-expressing VV [2]. We found no significant differences in the concentrations of radioactivity in the blood, liver, spleen, kidney, lung, brain, or bone marrow (femur). At the early (4 h) time point (Fig. 4A), the control mice that received the EGFP-expressing VV exhibited a higher whole-body retention of radioactivity (data not shown) and had a correspondingly higher retained radioactivity in the ovary, stomach, and small intestine. This was likely a reflection of differences in ^{111}In -pentetreotide clearance and did not lead to nonspecific uptake in the tumors of these mice. At 24 h there was further elimination of radioactivity from the blood and normal tissues but the high concentrations of radioactivity in the kidneys persisted (Fig. 4B). At 24 h, only the tumors of mice injected with the SSTR2-expressing virus contained significantly higher concentrations of radioactivity than controls ($P < 0.0001$).

We calculated tumor-to-normal tissue ratios 24 h after ^{111}In -pentetreotide injection. For all tissues, the tumor-to-normal tissue ratio in mice inoculated with the SSTR2-expressing VV was three to six times higher than that of mice receiving the control virus (Fig. 4C). This is a

further indication of the tumor specificity of the virus and will be important in considering the potential toxicity of a virus–radiotracer combination to normal tissues. In the control mice, tumor-to-normal tissue ratios were around 1, reflecting the normal background biodistribution in soft tissues. The higher ratio seen in blood, brain, and femur was due to very low biodistribution in these tissues and likely reflects rapid clearance

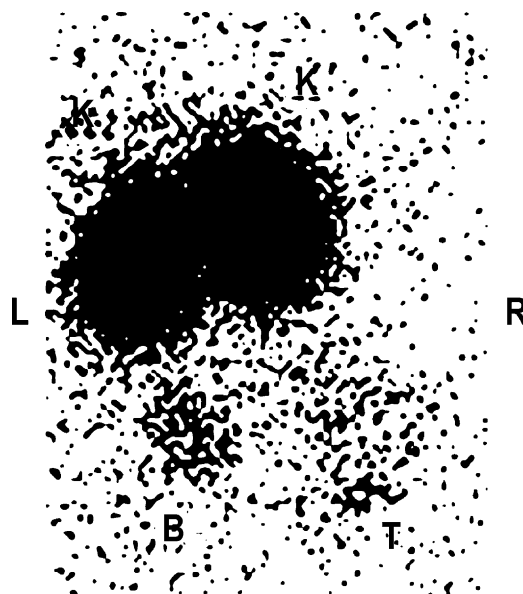


FIG. 3. Representative image of tumor-bearing athymic mouse 3 weeks after ip injection with vvDD-SSTR2 and 24 h after iv injection with ^{111}In -pentetreotide. Tumor (T) is visible on the right flank. Kidney (K) and bladder (B) are also visualized. The right (R) and left (L) sides of the mouse are indicated.

TABLE 1: Correlation of vaccinia/SSTR2 biodistribution with ¹¹¹In-pentetreotide biodistribution

Tissue	Tumor		Liver		Kidney	
	Virus: hSSTR2	EGFP	hSSTR2	EGFP	hSSTR2	EGFP
RT-PCR (SSTR2)	+	–	–	–	–	–
Viral titers (mean pfu/mg)	5.1×10^8	ND	1.9×10^2	ND	1.2×10^2	ND
ROI analysis (mean counts/pixel)	0.46*	0.26*	0.91	1.02	5.54	5.51
Biodistribution (%ID/gram)	0.94**	0.18**	0.37	0.37	6.91	7.53

ND, not done; ROI, region-of-interest.

* $P = 0.04$.

** $P < 0.0001$.

(blood) or filtering such as that by the blood–brain barrier or bone.

To confirm that ¹¹¹In-pentetreotide uptake was indeed a surrogate marker for SSTR2 expression, we performed RT-PCR on tumors and selected normal tissues (Fig. 5). Only the tumors infected with the VV carrying SSTR2 were positive for human SSTR2 (Fig. 5, lanes 1 to 3), while the tumors infected with the control virus were negative (lane 4). Although a small amount of SSTR2-expressing VV was detected in the liver and kidneys by plaque titering (Table 1), this was below the level of detection by RT-PCR. This is consistent with the visualization of SSTR2-infected tumors on the images and the higher tumor uptake of ¹¹¹In-pentetreotide in these tumors compared to tumors infected with the control VV. It further suggests that radiopharmaceutical localization was due to viral-mediated expression of SSTR2. Moreover, the minimal expression of SSTR2 in kidneys suggests that ¹¹¹In-pentetreotide accumulation in this organ was not mediated by viral-mediated expression of SSTR2. Importantly, the image ROI analysis correlated well with ¹¹¹In-pentetreotide biodistribution and the vaccinia-SSTR2 expression (Table 1).

DISCUSSION

A VV vector that expresses SSTR2 and permits molecular imaging using ¹¹¹In-pentetreotide will be advantageous for future cancer gene therapy trials. We have demonstrated specific uptake of ¹¹¹In-pentetreotide after VV-mediated delivery of SSTR2 both *in vitro* and *in vivo*. The unique properties of VV, which include the ability to localize selectively in tumors after systemic injection and high levels of gene expression, allow noninvasive molecular imaging of the vector delivery to tumors using a gamma camera.

The ability to track noninvasively vectors used in studies of gene therapy becomes critical as more human gene therapy trials come to fruition. It will be important to follow the location of the vector after delivery and the duration of its persistence. While several groups have developed vectors expressing reporter genes that encode receptors suitable for nuclear molecular imaging, limitations exist. Many of these vectors are small and cannot

incorporate both reporter genes for imaging and therapeutic genes. VV permits the insertion of up to 25 kb of foreign DNA, allowing for expression of several transgenes at once [36].

Second, and most important, nuclear imaging of viral gene expression has not been demonstrated after systemic administration of the vector [33,34]. In future trials of cancer gene therapy it will not be feasible in all cases to inject the vector directly into the tumor. In patients with metastatic disease, a vector that can be injected systemically and tracked noninvasively will be ideal. Previously we have shown that systemic injections of VV via either the intravenous or the intraperitoneal route were equivalent and led to high gene expression in subcutaneous tumors but low levels in other tissues [2]. This study confirms those results with high expression of the SSTR2 gene in the tumors after intraperitoneal VV injection, allowing tumor imaging due to specific accumulation of ¹¹¹In-pentetreotide. These results were confirmed by tissue biodistribution studies, which also correlated very well with image region-of-interest analysis.

Somatostatin is a 14-amino-acid peptide hormone. Pentetreotide, a stable analog, has an extended half-life *in vivo* [18]. This greatly facilitates its use in imaging studies. The human SSTR2 has high affinity for pentetreotide, which is commonly used for receptor imaging after being radiolabeled with ¹¹¹In [17]. The recent development of ^{99m}Tc-depreotide for somatostatin receptor imaging may be even more attractive since ^{99m}Tc has optimal imaging properties for the gamma camera and is readily available in all nuclear medicine laboratories [37,38]. The recent development of new somatostatin receptor ligands that can be used for peptide receptor radionuclide therapy (e.g., ⁹⁰Y-DOTA-TOC) makes the VV system attractive for future development, as expression of SSTR2 may therefore be used for imaging and therapy [18]. While traditionally somatostatin receptors have been imaged by single-photon-emission computed tomography using ¹¹¹In-pentetreotide, analogs that can be used for positron-emission tomography (PET) have recently been developed [39,40]. This suggests that the somatostatin receptor will continue to be a valuable reporter in the future for molecular imaging of viral gene delivery and expression.

In addition to its role in molecular imaging, the SSTR2 may have an anti-tumor effect in its own right. Previous studies in which SSTR2 was stably transfected into cell lines demonstrated inhibition of cell growth likely due to an autocrine negative feedback loop [41]. Distant bystander effects were also seen. The SSTR2 has also been transferred to non-SSTR2-expressing cell lines using adenoviral-mediated gene transfer [42]. Tumor growth inhibition was shown to be due to an increase in apoptosis.

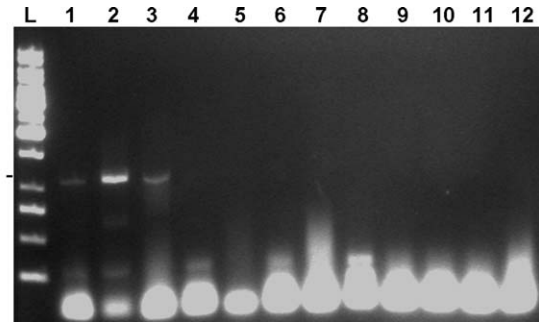
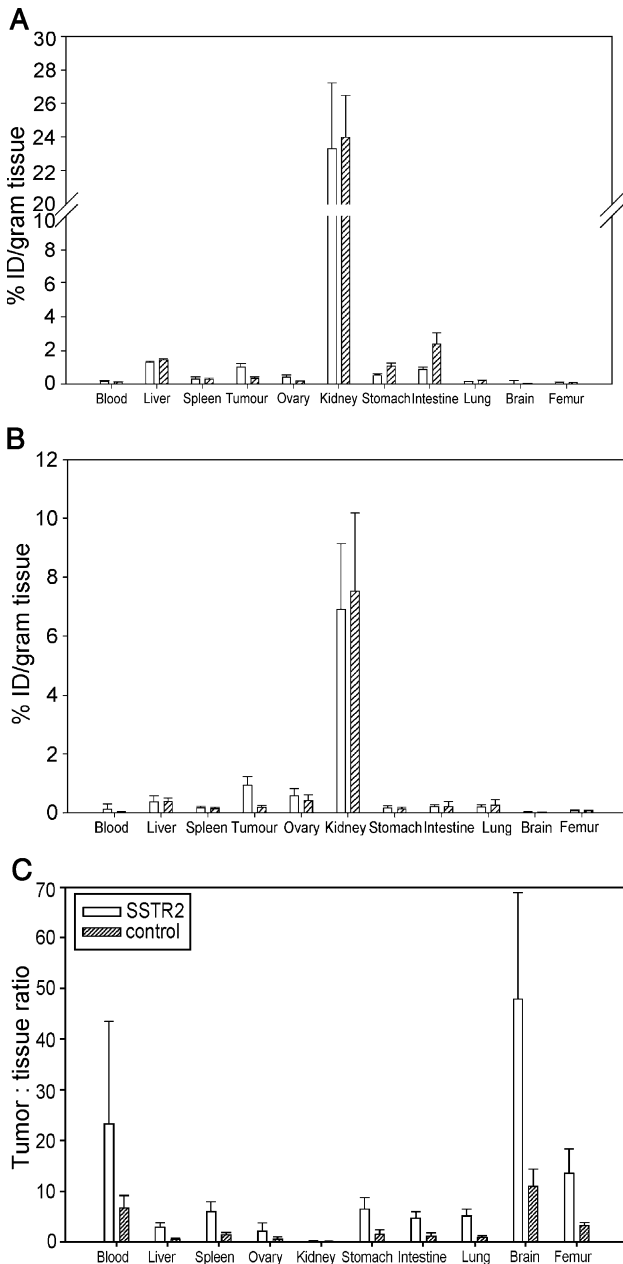


FIG. 5. RT-PCR analysis of total RNA purified from tumors (lanes 1–4), livers (lanes 5–8), and kidneys (lanes 9–12) of mice injected with vvDD-SSTR2 or the control virus vvDD-GFP (lanes 1–3, 5–7, 9–11). Primers for the SSTR2 gene amplify a 1100-bp segment in vvDD-SSTR2-infected tumors (lanes 1–3) but no band is amplified from the control virus (lane 4) or any other organs (lanes 5 to 12). L, 1 kb ladder.

There are some limitations to molecular imaging of viral gene delivery and expression using the somatostatin receptor. Renal uptake of ^{111}In -pentetreotide may impair the ability to visualize nearby tumors in the peritoneal cavity, but it has been previously shown [35] that this can be decreased by administration of positively charged, non-biologically active D-amino acids such as D-lysine before and during the administration of the radiotracer. D-Lysine administered iv can decrease the nonspecific uptake in the kidney by up to 50% [35].

Second, concerns have been raised about the ability to deliver reporter genes encoding receptors with oncolytic vectors [43]. Potentially the vector may act to lyse the cell prior to any reporter activity being noted. We have not encountered any difficulties and indeed we were able to image our vector for at least 3 weeks postinjection. Presumably the system is rapidly evolving but there remain sufficient live cells expressing the reporter to image the tumor. Nevertheless, we expect that as the virus eradicates the tumor we will see a decrease in image intensity.

FIG. 4. (A) ^{111}In -Pentetreotide biodistribution 4 h after iv (tail vein) injection into athymic mice bearing subcutaneous MC38 colon CA xenografts on the right flank, previously injected with the SSTR2-expressing vaccinia virus or EGFP-expressing control virus. Tumor had significantly ($P = 0.01$) higher radioactivity in mice infected with vvDD-SSTR2 (open bars) compared to vvDD-GFP (lined bars). No significant difference was seen in the blood, liver, spleen, kidney, lung, brain, or femur. The mice receiving the vvDD-GFP had greater radioactivity in ovary, stomach, and intestine, which diminished at 24 h. (B) ^{111}In -Pentetreotide biodistribution 24 h after injection. Tumor had significantly ($P < 0.0001$) higher uptake in athymic mice infected with vvDD-SSTR2 (open bars) compared to vvDD-GFP (lined bars). No significant difference was seen in the blood, liver, spleen, ovary, kidney, stomach, intestine, lung, brain, or femur. (C) Tumor-to-normal tissue ratios 24 h after injection with ^{111}In -pentetreotide into athymic mice previously injected with the SSTR2-expressing vaccinia virus or EGFP-expressing control virus. For all organs tested the tumor-to-normal ratios were three- to sixfold higher in the mice receiving the SSTR2-expressing virus.

The results of this study demonstrate (a) the correct processing of a human cell surface SSTR2 expressed by VV, (b) specific cellular uptake *in vitro* of ^{111}In -pentetreotide in cancer cells after infection with the SSTR2-expressing VV, (c) tumor-specific imaging with ^{111}In -pentetreotide after systemic delivery of VV, and (d) the ability to repetitively image the tumors over a 3-week period. The images obtained of tumors less than 1 cm in diameter demonstrate the potential of using VV as a systemic vector for tumor gene therapy, allowing non-invasive tracking of the vector. Future studies will be performed to optimize these results, including determining the most sensitive time to administer the radiopharmaceutical relative to virus injection. In addition, alternative receptor/radiopharmaceutical probe systems (e.g., dopamine DR2/ ^{123}I -IBF or ^{11}C -raclopride) and imaging technologies (e.g., PET and fluorescence imaging) are being explored to extend this highly promising strategy for visualizing the delivery and expression of viral gene therapy vectors.

MATERIALS AND METHODS

Cell lines and vaccinia viruses. The cell lines CV1 (monkey kidney fibroblasts) and MC38 (murine colon cancer) have been previously described [3]. AR4-2J (ATCC, Manassas, VA, USA) is a rat pancreatic tumor cell line that naturally expresses SSTR2 [44] and is used as a positive control. The recombinant (WR strain) VV vSC20, a kind gift from Dr. Bernard Moss, NIAID, NIH [45] and vvDD-GFP [3] were used in these experiments.

Creation of vaccinia virus expressing the human somatostatin receptor. The SSTR2 was cloned from a human kidney cancer specimen (Urology Branch, NCI, NIH) using standard techniques [46]. The sense primer was designed to contain an upstream coding sequence for the VV synthetic late promoter [47]. The product was sequenced and recombined into our parental vaccinia vSC20 using standard techniques [48]. The virus was expanded in CV1 cells and purified.

Reverse transcription polymerase chain reaction. CV1 cells were infected with the SSTR2 expressing VV or control VV at an m.o.i. of 1. When complete cytopathic effect was seen, the cells were harvested and RNA was extracted (RNeasy; Qiagen, Santa Clarita, CA, USA). Contaminating DNA was removed (DNA-free; Ambion, Austin, TX, USA) and a standard RT-PCR was performed using the Access RT-PCR system (Promega, Madison, WI, USA). Primers specific to SSTR2 or to β -actin (RT control) were used (SSTR2, sense 5'-GATCAAGCTT-TTTTTTTTTTTTTTTTGGCATATAAATGGACATGGCGGATGAGCC-3', antisense 5'-GATCTCAGATACTGGTTTGGAGGT-3'; β -actin, sense 5'-TGTGATGGTGGGAATGGGTCAAG-3', antisense 5'-TTGATGTCACGCAC-GATTTC-3'). In brief, 1 μg of the VV RNA, 2.5 μl of each primer (20 μM), 1 μl of dNTPs (10 mM), 5 units of *tfl* DNA polymerase, 5 units of AMV reverse transcriptase, 3 μl of MgSO_4 (25 mM), 10 μl of 5 \times buffer, and nuclease-free water to 50 μl final volume was added. PCR parameters consisted of 45 min first-strand synthesis (48°C) and then 2 min denaturing (94°C), 30 s annealing (55°C), and 2 min extension (72°C) for 40 cycles (GeneAmp PCR System 9700; Perkin-Elmer, Norwalk, CT, USA). Reactions without AMV-RT were done to control for DNA contamination.

Immunostaining for SSTR2. Confluent CV1 cells in six-well plates were infected with the SSTR2-expressing VV or controls. When viral plaques

were observed the cells were immunostained as previously described [48]. The rabbit polyclonal antibody against the human somatostatin type 2 receptor (Biogenesis, Kingston, NH, USA) was used at a 1/500 dilution. The secondary anti-rabbit HRP was used at a 1/1000 dilution. The TMB substrate kit for peroxidase (Vector Laboratories, Burlingame, CA, USA) was used as directed.

^{111}In -Pentetreotide binding assay. Confluent CV1 cells in six-well plates were infected with the SSTR2-expressing VV at an m.o.i. of 1, a control VV containing the EGFP gene, or no virus. After 18 h the cells were washed in buffer (serum-free DMEM with 0.5% BSA) and then incubated with ^{111}In -pentetreotide (25 $\mu\text{Ci}/32$ ng; Mallinckrodt Medical, St. Louis, MO, USA), 1 mM phenanthroline (Sigma Chemical Co., St. Louis, MO, USA), and 1/1000 vol proteinase cocktail (Sigma Chemical Co.) for 1 h at 37°C. Cells were then washed with buffer $\times 2$, collected, and read in a gamma counter gated for 100–500 keV. For the competitive binding assay MC38 cells were infected with the SSTR2-expressing VV or control virus at an m.o.i. of 1. After 18 h, cells were incubated in 1.5-ml Eppendorf tubes (Diamed Lab Supplies, Inc., Mississauga, ON, Canada) with 5 μCi of ^{111}In -pentetreotide plus increasing doses (0- to 1000-fold excess) of nonradiolabeled pentetreotide for 1 h at 37°C. Cells were then washed $\times 2$, recovered by centrifugation, and counted in a gamma counter.

Mice. Six-week-old female athymic (nu/nu) mice were obtained from Cedarlane Laboratories (Montreal, QC, Canada) or the National Institutes of Health Small Animal Facility (Frederick, MD, USA). They were housed under standard conditions and given food and water *ad lib*. All animal studies were done under protocols approved by the Animal Resource Centre, University Health Network, Toronto, Canada, or the Animal Care and Use Subcommittee of the Animal Sciences Branch, National Cancer Institute.

***In vivo* imaging and biodistribution.** ^{111}In -Pentetreotide (OctreoScan) was purchased from Mallinckrodt Medical. The radiopharmaceutical was prepared according to the manufacturer's instructions. All doses were measured on a Capintec Radioisotope Calibrator 12R (Capintec, Inc., Ramsey, NJ, USA). The radiochemical purity was 93–98%. The specific activity of the radiopharmaceutical was 7.9–11.6 MBq/ μg (200–300 $\mu\text{Ci}/\mu\text{g}$).

When subcutaneous MC38 murine colon cancer xenografts were 5 to 7 mm in size, 10^9 pfu of the SSTR2 or control virus was injected ip. Six days later groups of four to six mice were injected with 5.5 MBq (150 μCi ; 0.5–0.7 μg) each of ^{111}In -pentetreotide. Three to six mice from each group were anesthetized using a mixture of ketamine (90 mg/kg), xylazine (10 mg/kg), and acepromazine (2.5 mg/kg) sq and imaged approximately 4 and 24 h after radiopharmaceutical administration. Images were obtained using an ADAC TransCam gamma camera (ADAC Laboratories, Inc., Milpitas, CA, USA) with pinhole collimator (4-mm aperture) and online computer and proprietary software (Pegasys, version 4.2). Dorsal views were acquired on a 256 \times 256 matrix using a 30% window centered on the 247-keV photo peak of ^{111}In . Images were acquired for 25 to 30 min and typically a mean of 50,000 counts was obtained. All images were normalized to kidney uptake prior to analysis.

Standard manual ROI analyses were drawn around visualized organs including tumor, kidney, liver, mediastinum, brain, femur, and whole body. Background analysis was taken from a region outside of the animal. Tumor uptake was normalized to the kidney uptake prior to analysis and background correction performed. The mean counts per pixel were recorded for each ROI and compared to the results obtained from the tissue biodistribution studies.

The same groups of four to six mice each were used for tissue biodistribution experiments. The animals were sacrificed early (6–8 h) or late (24 h) post-injection of the radiopharmaceutical by cranial-cervical dislocation. Mice were bled by intracardiac puncture and then tissues including blood, liver, spleen, tumor, ovary, kidney, stomach, intestine, lung, brain, and bone were weighed (g) and counted using a Cobra Quantum Automated Gamma Counting System (Packard Instrument Co., Meriden, CT, USA), Model 5003 (single 3-in. detector; 15–2000 keV). The

windows were set to include the 150–190 and 230–270 keV photopeaks of ^{111}In . By counting a known standard of the injected dose, the radioactivity uptake in each tissue was determined as percentage injected dose/g (% ID/g).

RT-PCR and plaque titering. Tissues from tumors, livers, and kidneys were snap-frozen in liquid nitrogen. RNA was obtained using TRIzol reagent (Invitrogen Canada, Inc., Burlington, ON, Canada). RT-PCR for expression of SSTR2 was performed as described above. The remaining tissues were homogenized in HBSS and plaque-titred on confluent CV1 cells as previously described [48].

Statistics. Statistical analysis was performed using the Student *t* test when appropriate. All statistics were generated using StatView Software (Abacus Concepts, Inc., Berkeley, CA, USA), and *P* values <0.05 were considered significant.

ACKNOWLEDGMENTS

The authors thank Karen Wong (Department of Nuclear Medicine, NIH) for help with the biodistribution studies. This work was supported in part by grants from the Ontario Cancer Research Network and the University of Toronto Deans Fund to J.A.M.

RECEIVED FOR PUBLICATION JUNE 2, 2004; ACCEPTED JUNE 9, 2004.

REFERENCES

- Puhlmann, M., Gnant, M., Brown, C. K., Alexander, H. R., and Bartlett, D. L. (1999). Thymidine kinase deleted vaccinia virus expressing purine nucleoside phosphorylase as a vector for tumor directed gene therapy. *Hum. Gene Ther.* **10**: 649–657.
- McCart, J. A., et al. (2000). Complex interactions between the replicating oncolytic effect and the enzyme/prodrug effect of vaccinia-mediated tumor regression. *Gene Ther.* **7**: 1217–1223.
- McCart, J. A., et al. (2001). Systemic cancer therapy with a tumor selective vaccinia virus mutant lacking thymidine kinase and vaccinia growth factor genes. *Cancer Res.* **61**: 8751–8757.
- Kohn, S., Nagy, J. A., Dvorak, H. F., and Dvorak, A. M. (1992). Pathways of macromolecular tracer transport across venules and small veins: structural basis for the hyperpermeability of tumor blood vessels. *Lab. Invest.* **67**: 596–607.
- Goede, V., Schmidt, T., Kimmina, S., Kozian, D., and Augustin, H. G. (1998). Analysis of blood vessel maturation processes during cyclic ovarian angiogenesis. *Lab. Invest.* **78**: 1385–1394.
- Bhaumik, S., and Gambhir, S. S. (2002). Optical imaging of Renilla luciferase reporter gene expression in living mice. *Proc. Natl. Acad. Sci. USA* **99**: 377–382.
- Honigman, A., et al. (2001). Imaging transgene expression in live animals. *Mol. Ther.* **4**: 239–249.
- Adams, J. Y., et al. (2002). Visualization of advanced human prostate cancer lesions in living mice by targeted gene transfer vector and optical imaging. *Nat. Med.* **8**: 891–896.
- Wu, J. C., Inubushi, M., Sundaresan, G., Schelbert, H. R., and Gambhir, S. S. (2002). Optical imaging of cardiac reporter gene expression in living rats. *Circulation* **105**: 1631–1634.
- Bouvet, M., et al. (2002). Real-time optical imaging of primary tumor growth and multiple metastatic events in a pancreatic cancer orthotopic model. *Cancer Res.* **62**: 1534–1540.
- Diehn, F. E., et al. (2002). Noninvasive fluorescent imaging reliably estimates biomass in vivo. *BioTechniques* **33**: 1250–1255.
- Ray, P., Wu, A. M., and Gambhir, S. S. (2003). Optical bioluminescence and positron emission tomography imaging of a novel fusion reporter gene in tumour xenografts in living mice. *Cancer Res.* **63**: 1160–1165.
- Tjuvajev, J. G., et al. (1998). Imaging herpes virus thymidine kinase gene transfer and expression by positron emission tomography. *Cancer Res.* **58**: 4333–4341.
- Gambhir, S. S., et al. (1999). Imaging adenoviral-directed reporter gene expression in living animals with positron emission tomography. *Proc. Natl. Acad. Sci. USA* **96**: 2333–2338.
- Inubushi, M., et al. (2003). Positron-emission tomography reporter gene expression imaging in rat myocardium. *Circulation* **107**: 326–332.
- Jacobs, A., et al. (2001). Positron emission tomography-based imaging of transgene expression mediated by replication-conditional, oncolytic herpes simplex type 1 mutant vectors in vivo. *Cancer Res.* **61**: 2983–2995.
- Slooter, G. D., et al. (2001). Somatostatin receptor imaging, therapy and new strategies in patients with neuroendocrine tumours. *Br. J. Surg.* **88**: 31–40.
- Breeman, W. A. P., et al. (2001). Somatostatin receptor-mediated imaging and therapy: basic science, current knowledge, limitations and future perspectives. *Eur. J. Nucl. Med.* **28**: 1421–1429.
- Rogers, B. E., et al. (1999). In vivo localization of [^{111}In]-DTPA-D-Phe1-octreotide to human ovarian tumor xenografts induced to express the somatostatin receptor subtype 2 using an adenoviral vector. *Clin. Cancer Res.* **5**: 383–393.
- MacLaren, D. C., et al. (1999). Repetitive, non-invasive imaging of the dopamine D2 receptor as a reporter gene in living animals. *Gene Ther.* **6**: 785–791.
- Sun, X., et al. (2001). Quantitative imaging of gene induction in living animals. *Gene Ther.* **8**: 1572–1579.
- Liang, Q., et al. (2001). Noninvasive, quantitative imaging in living animals of a mutant dopamine D2 receptor reporter gene in which ligand binding is uncoupled from signal transduction. *Gene Ther.* **8**: 1490–1498.
- Cho, J.-Y., et al. (2002). In vivo imaging and radioiodine therapy following sodium iodide symporter gene transfer in animal model of intracerebral gliomas. *Gene Ther.* **9**: 1139–1145.
- Groot-Wassink, T., Aboagye, E. O., Glaser, M., Lemoine, N. R., and Vassaux, G. (2002). Adenovirus biodistribution and noninvasive imaging of gene expression in vivo by positron emission tomography using human sodium/iodide symporter as reporter gene. *Hum. Gene Ther.* **13**: 1723–1735.
- Barton, K. N., et al. (2003). GENIS: gene expression of sodium iodide symporter for noninvasive imaging of gene therapy vectors and quantification of gene expression in vivo. *Mol. Ther.* **8**: 508–518.
- Auricchio, A., et al. (2003). In vivo quantitative noninvasive imaging of gene transfer by single-photon emission computerized tomography. *Hum. Gene Ther.* **14**: 255–261.
- de Vries, E. F. J., and Vaalburg, W. (2002). Positron emission tomography: measurement of transgene expression. *Methods* **27**: 234–241.
- Alauddin, M. A., Shahinian, A., Kundu, R. K., Gordon, E. M., and Conti, P. S. (1999). Evaluation of 9-[(3- ^{18}F -fluoro-1-hydroxy-2-propoxy)methyl]guanine ([^{18}F]-FHPG) in vitro and in vivo as a probe for PET imaging of gene incorporation and expression in tumors. *Nucl. Med. Biol.* **26**: 371–376.
- Zinn, K. R., et al. (2002). Gamma camera dual imaging with a somatostatin receptor and thymidine kinase after gene transfer with a bicistronic adenovirus in mice. *Radiology* **223**: 417–425.
- Hemminki, A., et al. (2001). An adenovirus with enhanced infectivity mediates molecular chemotherapy of ovarian cancer cells and allows imaging of gene expression. *Mol. Ther.* **4**: 223–231.
- Chaudhuri, T. R., Rogers, B. E., Buchsbaum, D. J., Mountz, J. M., and Zinn, K. R. (2001). A noninvasive reporter system to image adenoviral-mediated gene transfer to ovarian cancer xenografts. *Gynecol. Oncol.* **83**: 432–438.
- Zinn, K. R., Buchsbaum, D. J., Chaudhuri, T. R., Mountz, J. M., Grizzle, W. E., and Rogers, B. E. (2000). Noninvasive monitoring of gene transfer using a reporter receptor imaged with a high affinity peptide radiolabeled with $^{99\text{m}}\text{Tc}$ or ^{188}Re . *J. Nucl. Med.* **41**: 887–895.
- Hemminki, A., et al. (2002). In vivo molecular chemotherapy and noninvasive imaging with an infectivity-enhanced adenovirus. *J. Natl. Cancer Inst.* **94**: 741–749.
- Rogers, B. E., Chaudhuri, T. R., Reynolds, P. N., Manna, D. D., and Zinn, K. R. (2003). Non-invasive gamma camera imaging of gene transfer using an adenoviral vector encoding an epitope-tagged receptor as a reporter. *Gene Ther.* **10**: 105–114.
- Bernard, B. F., et al. (1997). D-Lysine reduction of indium-111 octreotide and yttrium-90 octreotide renal uptake. *J. Nucl. Med.* **38**: 1929–1933.
- Moss, B. (1991). Vaccinia virus: a tool for research and vaccine development. *Science* **252**: 1662–1667.
- Virgolini, I., et al. (2001). New trend in peptide receptor radioligands. *Q. J. Nucl. Med.* **45**: 153–159.
- Menda, Y., and Kahn, D. (2002). Somatostatin receptor imaging of non-small cell lung cancer with $^{99\text{m}}\text{Tc}$ depreotide. *Semin. Nucl. Med.* **32**: 92–96.
- Uger, O., et al. (2002). Ga-66 labeled somatostatin analogue DOTA-D-Phe1-Tyr3-octreotide as a potential agent for positron emission tomography imaging and receptor mediated internal radiotherapy of somatostatin receptor positive tumors. *Nacl. Med. Biol.* **29**: 147–157.
- Henze, M., et al. (2001). PET imaging of somatostatin receptors using [^{68}Ga]-DOTA-D-Phe1-Tyr3-octreotide: first results in patients with meningiomas. *J. Nucl. Med.* **42**: 1053–1056.
- Rochaix, P., et al. (1999). Gene therapy for pancreatic carcinoma: local and distant antitumor effects of somatostatin receptor *sst2* gene transfer. *Hum. Gene Ther.* **10**: 995–1008.
- Vernejoul, F., et al. (2002). Antitumor effect of in vivo somatostatin receptor subtype 2 gene transfer in primary and metastatic pancreatic cancer models. *Cancer Res.* **62**: 6124–6131.
- Le, L. P., Davydova, J. G., Yamamoto, M., and Curiel, D. T. (2003). Fluorescently labeled adenovirus with IX-EGFP for monitoring conditionally replicative adenovirus replication and distribution. *Proc. Am. Assoc. Cancer Res.* **44**: 1320
- Froidevaux, S., Hintermann, E., Török, M., Mäcke, H. R., Belinger, C., and Eberle, A. N.

- (1999). Differential regulation of somatostatin receptor type 2 (sst 2) expression in A24-2J tumor cells implanted into mice during octreotide treatment. *Cancer Res.* **59**: 3652–3657.
45. Buller, R. M. L., Chakrabarti, S., Cooper, J. A., Twardzik, D. R., and Moss, B. (1988). Deletion of the vaccinia virus growth factor gene reduces virus virulence. *J. Virol.* **62**: 866–874.
46. Kingston, R. E. (1998). Preparation and analysis of RNA. In *Current Protocols in Molecular Biology* (F. M. Ausubel, R. E. Kingston, R. Kinston, D. D. Moore, J. G. Seidman, J. A. Smith, and K. Struhl, Eds.), pp.4.0.1-4.10.11. Greene/Wiley Interscience, New York.
47. Davison, A. J., and Moss, B. (1989). Structure of vaccinia virus late promoters. *J. Mol. Biol.* **210**: 771–784.
48. Earl, P. L. and Moss B. (1998). Expression of proteins in mammalian cells using vaccinia viral vectors. In *Current Protocols in Molecular Biology* (F. M. Ausubel, R. E. Kingston, R. Kinston, D. D. Moore, J. G. Seidman, J. A. Smith, and K. Struhl, Eds.), pp. 16.15.1-16.18.11. Greene/Wiley Interscience, New York.